Performance Analysis and Design Optimization of LDPC-Coded MIMO OFDM Systems

Ben Lu, *Member, IEEE*, Guosen Yue, *Student Member, IEEE*, and Xiaodong Wang, *Member, IEEE*

***Abstract*—We consider the performance analysis and design optimization of low-density parity check (LDPC) coded multiple-input multiple-output (MIMO) orthogonal frequency-division multiplexing (OFDM) systems for high data rate wireless transmission. The tools of density evolution with mixture Gaussian approximations are used to optimize irregular LDPC codes and to compute minimum operational signal-to-noise ratios (SNRs) for ergodic MIMO OFDM channels. In particular, the optimization is done for various MIMO OFDM system configurations, which include a different number of antennas, different channel models, and different demodulation schemes; the optimized performance is compared with the corresponding channel capacity. It is shown that along with the optimized irregular LDPC codes, a turbo iterative receiver that consists of a soft maximum *a posteriori* (MAP) demodulator and a belief-propagation LDPC decoder can perform within 1 dB from the ergodic capacity of the MIMO OFDM systems under consideration. It is also shown that compared with the optimal MAP demodulator-based receivers, the receivers employing a low-complexity linear minimum mean-square-error soft-interference-cancellation (LMMSE-SIC) demodulator have a small performance loss ($<$ 1dB) in spatially uncorrelated MIMO channels but suffer extra performance loss in MIMO channels with spatial correlation. Finally, from the LDPC profiles that already are optimized for ergodic channels, we heuristically construct small block-size irregular LDPC codes for outage MIMO OFDM channels; as shown from simulation results, the irregular LDPC codes constructed here are helpful in expediting the convergence of the iterative receivers.**

***Index Terms*—Code design, density evolution, ergodic capacity, LDPC, LMMSE-SIC, MAP, MIMO, mixture Gaussian, OFDM, outage capacity.**

I. Introduction

ONE of the ambitious design goals of fourth–generation (4G) wireless cellular systems is to reliably provide very high data rate transmission, for example, around 100 Mb/s peak rate for downlink and around 30 Mb/s sum rate for uplink transmission. Due to its higher rate requirement, the downlink transmission is especially considered to be a bottleneck in system design. In this paper, we demonstrate the feasibility of *downlink transmission* in 4G wireless systems through the physical-layer (PHY) design and optimization of low-density parity check (LDPC) coded wireless multiple-input multiple-output (MIMO) orthogonal frequency-division multiplexing (OFDM) communications. In the considered systems, different users access the downlink channels in a time-division multiple accessing (TDMA) manner, dynamic with a certain scheduling scheme [1]. Compared with other alternative solutions, the MIMO-OFDM-TDMA downlink transmission proposed here attempts to balance between high rate transmission and low receiver complexity of mobile devices, where the former primarily counts on the LDPC-coded MIMO techniques, and the latter is owing to the orthogonal structure of OFDM-TDMA.

A large number of works on the physical-layer study of MIMO techniques has been done in the past decade. Various MIMO schemes could be distinguished by different design goals, for example, the BLAST systems [2] aimed at the highest data-rate or the orthogonal space-time block code (STBC) [3] aimed at the full transmit diversity. On the other hand, these MIMO schemes could also be categorized according to the different ways of making use of channel state information (CSI), for example, the space-time codes [4] that assume no CSI at transmitter side or the optimal eigen-beamforming [5] schemes that assume perfect CSI at transmitter. In this work, we restrict our attention to the schemes that require no CSI at transmitter and aim to achieve very high data rate. In particular, we focus on an LDPC-coded MIMO OFDM scheme proposed in [6] and [7].

In this paper, for a fixed target data rate (e.g., 100 Mb/s), we optimize and compare the performance of the LDPC-coded MIMO OFDM systems with different configurations. For a fair comparison, we adopt the quantity $\mathrm{SNR}_{\min\text{-}op}(\mathrm{dB}) - C^{-1}(R)(\mathrm{dB})$ as the performance measure, which reflects how many decibels the minimum operational $\mathrm{SNR}_{\min\text{-}op}$ is above the SNR required by the information theoretic channel capacity $C(\cdot)$ to support a target information rate R. We also remark that in this paper, the notion of *data rate* (in the unit of bits per second) will be differentiated from *information rate* (in the unit of bits per second per Hertz) when the bandwidth (in the unit of Hertz) is not specified or fixed. Specifically, we are interested in the following problems.

- *Different number of antennas:* We consider the MIMO system with N transmitter antennas and M receiver antennas. As a well-known result from information theory [5], [8], at high SNRs, a narrowband MIMO system can support a $m = \min(N, M)$ times higher information rate than that in single-antenna $(M = N = 1)$ systems. One may wonder whether in wideband transmission such a MIMO system is capable of providing the same data rate with one mth bandwidth required by a single-antenna system?

Manuscript received December 12, 2002; revised April 24, 2003. G. Yue and X. Wang were supported in part by the U.S. National Science Foundation under Grants CCR-0207550 and CCR-0225721 and by the U.S. Office of Naval Research under Grant N00014-03-1-0039. The associate editor coordinating the review of this paper and approving it for publication was Dr. Michael P. Fitz.

B. Lu is with the NEC Laboratories America, Princeton, NJ 08540 USA.

G. Yue is with the Department of Electrical Engineering, Texas A&M University, College Station, TX 77843 USA.

X. Wang is with the Department of Electrical Engineering, Columbia University, New York, NY 10027 USA.

Digital Object Identifier 10.1109/TSP.2003.820991

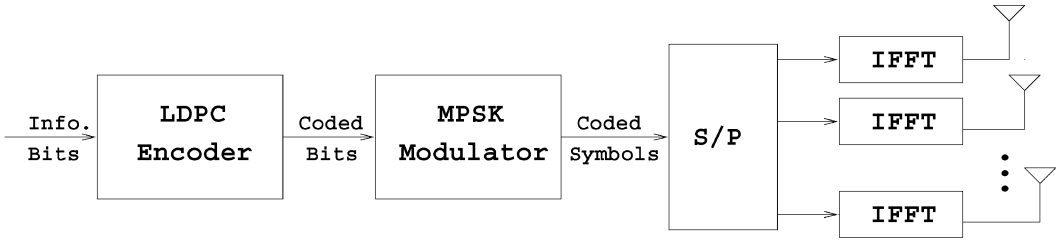

Fig. 1. Transmitter structure of an LDPC-coded MIMO OFDM system.

- *Different soft-input-soft-output (abbreviated as "soft") demodulation schemes:* We consider both the optimal maximum *a posteriori* (MAP) demodulator with a complexity at $\mathcal{O}(|\Omega|^N)$, where $|\Omega|$ is the constellation size of modulator, and N is the number of transmitter antennas; in addition, the suboptimal linear minimum mean-square-error based soft interference cancellation (LMMSE-SIC) demodulator with a complexity at $\mathcal{O}(|\Omega|^3)$. What is the performance penalty of applying LMMSE-SIC in LDPC-coded MIMO OFDM?
- *Different MIMO channel models:* We consider both the spatially uncorrelated MIMO channel model and the spatially correlated model. As a result shown by information theory [9], the channel capacity can be substantially reduced for spatially correlated MIMO channels. What is the impact of spatial correlation on the LDPC code design and optimization?

Many previous works have addressed the different aspects of the above problems, e.g., [2], [7], [8], [10], and [11]. However, only very lately, the work in [7] studied the LDPC code design in the MIMO systems under the framework of turbo iterative signal processing and decoding via the tools of EXIT charts. In this work, for each system configuration described above, we employ the techniques of density evolution with mixture Gaussian approximations [12]–[15] to design and optimize the irregular LDPC codes, as well as to compute the $\text{SNR}_{\min\,.op}$ for ergodic MIMO OFDM channels. Furthermore, from the LDPC profiles that are optimized for the ergodic channels, we heuristically construct small block-size irregular LDPC codes for outage MIMO OFDM channels. In the end, quantitative results from both the density evolution analysis/design and computer simulations give rise to a number of useful observations and conclusions in the design and optimization of the LDPC MIMO OFDM systems.

The paper is organized as follows. In Section II, we describe an LDPC-coded MIMO OFDM system with a brief summary of the system model and channel capacity of MIMO OFDM modulation and a brief background on the LDPC codes. In Section III, a turbo iterative receiver is introduced, with a brief review of the different demodulation schemes and the decoding scheme. In Section IV, we discuss the procedure of analyzing and optimizing the LDPC codes for MIMO OFDM systems. In Section V, the performance analysis and LDPC code optimization results for LDPC-coded MIMO OFDM systems with different system configurations are demonstrated and discussed. Section VI contains the conclusions.

II. System Description of LDPC Coded MIMO OFDM

We consider an LDPC-coded MIMO OFDM system with K subcarriers, N transmitter antennas, and M receiver antennas, signaling through frequency-selective fading channels. The transmitter structure is illustrated in Fig. 1. A block of k bits of information data is encoded by a rate $r = k/n$ LDPC code. The output n coded bits are interleaved. The interleaved bits are modulated by quadrature amplitude modulated (QAM) constellation Ω into a block of $n/\log_2|\Omega|$ QAM symbols. During each OFDM slot, NK out of the total $n/\log_2|\Omega|$ QAM symbols are transmitted from K OFDM subcarriers and N transmitter antennas simultaneously. Due to the inherent random structure of LDPC codes, the NK symbols can be mapped to K subcarriers and N transmitter antennas in any order. Without loss of generality, we assume $(n/\log_2|\Omega|)/(NK) = \tilde{n}$, i.e., the total block of QAM symbols is transmitted in $\tilde{n}$ OFDM slots.

Note that in Fig. 1, LDPC could also be replaced by other error-control codes such as Turbo codes; however, the relatively low and scalable decoding complexity and the freedom for code optimization make LDPC codes a more favorable candidate.

A. MIMO OFDM Modulation

Consider a quasistatic block fading model for the studied MIMO OFDM modulation, as in Fig. 2. It is assumed that the fading channels remain static during each OFDM slot but vary independently from one OFDM slot to another. Furthermore, for practical MIMO OFDM systems with spatial (antenna) correlations, the frequency domain channel response matrix at the kth $(k = 0, \ldots, K-1)$ subcarrier and the pth $(p = 0, \ldots, \tilde{n}-1)$ OFDM slot is given by [16]

$$\boldsymbol{H}[p,k] = \sum_{l=0}^{L-1} \boldsymbol{R}_l^{1/2} \boldsymbol{H}_l[p] \boldsymbol{S}_l^{1/2} \exp\left(\frac{-j2\pi lk}{K}\right) \tag{1}$$

where $\boldsymbol{R}_l = \boldsymbol{R}_l^{1/2}\boldsymbol{R}_l^{1/2}$, and $\boldsymbol{S}_l = \boldsymbol{S}_l^{1/2}\boldsymbol{S}_l^{1/2}$ represent the receive and transmit spatial-correlation matrices, which are determined by the spacing and the angle spread of MIMO antennas, as will be explained in Section V-C. L is the number of resolvable paths of the frequency-selective fading channels; $\boldsymbol{H}_l[p]$ is the matrix with entries being independent and identically distributed (i.i.d.) circularly symmetric complex Gaussian, distributed as $\sim\mathcal{N}_c(0, \beta_l^2)$, and is assumed to be independent for different l and different p; in addition, the power of $\boldsymbol{H}_l[p], \forall l$ is normalized by letting $\sum_{l=0}^{L-1} \beta_l^2 \equiv 1$.

Assume proper cyclic insertion and sampling, the MIMO OFDM system with K subcarriers decouples frequency-selective channels into K correlated flat-fading channels with the following input–output relation:

$$\boldsymbol{y}[p,k] = \sqrt{\frac{\text{SNR}}{N}}\boldsymbol{H}[p,k]\boldsymbol{x}[p,k] + \boldsymbol{z}[p,k]$$
$$k = 0, \ldots, K-1, \quad p = 0, \ldots, \tilde{n}-1 \tag{2}$$

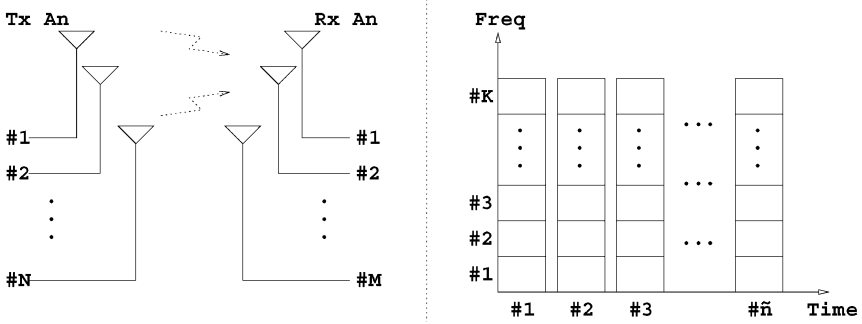

Fig. 2. Quasistatic block-fading MIMO OFDM channel model. For each OFDM slot, the fading channel responses remain static but are correlated in different OFDM subcarriers. For different OFDM slots, the fading channel responses are independent. [Note that in Fig. 2, the spatial relation of fading channels associated with different transmit-receive-antenna-pairs is defined through $\boldsymbol{R}_l$ and $\boldsymbol{S}_l$ in (1)].

where $\boldsymbol{H}[p,k] \in \mathcal{C}^{M\times N}$ is the matrix of complex channel frequency responses defined in (1); $\boldsymbol{x}[p,k] \in \Omega^N$ and $\boldsymbol{y}[p,k] \in \mathcal{C}^M$ are, respectively, the transmitted signals and the received signals at the kth subcarrier and the pth slot; $\boldsymbol{z}[p,k] \in \mathcal{C}^M$ is the additive noise with i.i.d. entries $\boldsymbol{z}[p,k] \sim \mathcal{N}_c(0,\boldsymbol{I})$; and SNR denotes the average signal-to-noise ratio at each receiver antenna. Note that in this work, only the fixed/deterministic (in contrast to variable/adaptive) signal constellation Ω is considered, and its averaged power is normalized to be one.

With no channel state information (CSI) at the transmitter side, the channel capacity for the above MIMO OFDM modulation has been studied in [5] and [8]. Assuming Gaussian signaling (i.e., $\Omega \to \mathcal{C}$) for MIMO OFDM channels with infinite fading channel observations (i.e, $\tilde{n} \to \infty$), the *ergodic capacity* is given by (3), shown at the bottom of the page, where ^{H} denotes the Hermitian transpose; the expectation is taken over random channel states $\mathcal{H}$, with $\mathcal{H} \triangleq \{\boldsymbol{H}[p,k]\}_{p,k}$; and $\mathcal{I}_{|\mathcal{H}}(\text{SNR})$ is the instantaneous mutual information conditioned on $\mathcal{H}$. For MIMO OFDM channels with finite fading channel observations (i.e, $\tilde{n} \ll \infty$), the *outage capacity/probability* is a more sensible measure. For a target information rate R, the outage probability is given by

$$P_{\text{out}}(R,\text{SNR}) = P(\mathcal{I}_{|\mathcal{H}}(\text{SNR}) < R). \tag{4}$$

In practice, the transmitted signals usually take values from constraint constellation, i.e., $\boldsymbol{x} \in \Omega^N$. In this case, following [17], the mutual information is computed instead as (5), shown at the bottom of the page, where the expectation is taken over random noise vector $\boldsymbol{z} \sim \mathcal{N}_c(0,\boldsymbol{I})$.

B. Low-Density Parity Check (LDPC) Codes

A low density parity check (LDPC) code is a linear block code specified by a very sparse parity check matrix. The parity check matrix $\boldsymbol{P}$ of a *regular* (n,k,s,t) LDPC code of rate $r = k/n$ is a $(n-k)\times n$ matrix, which has s ones in each column and $t > s$ ones in each row, where $s \ll n$, and the ones are typically placed at random in the parity check matrix. When the number of ones in every column is not the same, the code is known as an *irregular* LDPC code. Although deterministic construction of LDPC codes is possible, in this paper, we consider only pseudo-random constructions.

The code with parity check matrix $\boldsymbol{P}$ can be represented by a bipartite graph that consists of two types of nodes—variable nodes and check codes. Each code bit is a variable node, whereas each parity check or each row of the parity check matrix represents a check node. An edge in the graph is placed between variable node i and check node j if $P_{j,i} = 1$. That is, each check node is connected to code bits whose sum modulo-2 should be zero. Irregular LDPC codes are specified by two polynomials $\lambda(x) = \sum_{i=1}^{d_{l\max}} \lambda_i x^{i-1}$ and $\rho(x) = \sum_{i=1}^{d_{r\max}} \rho_i x^{i-1}$, where λ_i is the fraction of edges in the bipartite graph that are connected to variable nodes of degree i, and ρ_i is the fraction of edges that are connected to check nodes of degree i. Equivalently, the degree profiles can also be specified from the node perspective, i.e., two polynomials $\tilde{\lambda}(x) = \sum_{i=1}^{d_{l\max}} \tilde{\lambda}_i x^{i-1}$ and $\tilde{\rho}(x) = \sum_{i=1}^{d_{r\max}} \tilde{\rho}_i x^{i-1}$, where $\tilde{\lambda}_i$ is the fraction of variable nodes of degree i, and $\tilde{\rho}_i$ is the fraction of check nodes of degree i.

$$C_{erg}(\text{SNR}) \triangleq E\left\{ \underbrace{\frac{1}{K\tilde{n}} \sum_{k=0}^{K-1}\sum_{p=0}^{\tilde{n}-1} \left[\log_2 \det\left(\boldsymbol{I}_M + \frac{\text{SNR}}{N}\boldsymbol{H}[p,k]\boldsymbol{H}^H[p,k]\right)\right]}_{\mathcal{I}_{|\mathcal{H}}(\text{SNR})} \right\} \text{bits/Hz/s} \tag{3}$$

$$\mathcal{I}_{|\mathcal{H}}(\text{SNR}) = N\log_2|\Omega| - \frac{1}{K\tilde{n}|\Omega|^N} \times \sum_{k=0}^{K-1}\sum_{p=0}^{\tilde{n}-1}\sum_{j=0}^{|\Omega|^N-1} E\left\{ \log_2 \sum_{i=0}^{|\Omega|^N-1} \exp\left[-\left\| \sqrt{\frac{\text{SNR}}{N}}\boldsymbol{H}[p,k]\left(\boldsymbol{x}^j - \boldsymbol{x}^i\right) + \boldsymbol{z}\right\|^2 + \|\boldsymbol{z}\|^2 \right] \right\} \tag{5}$$

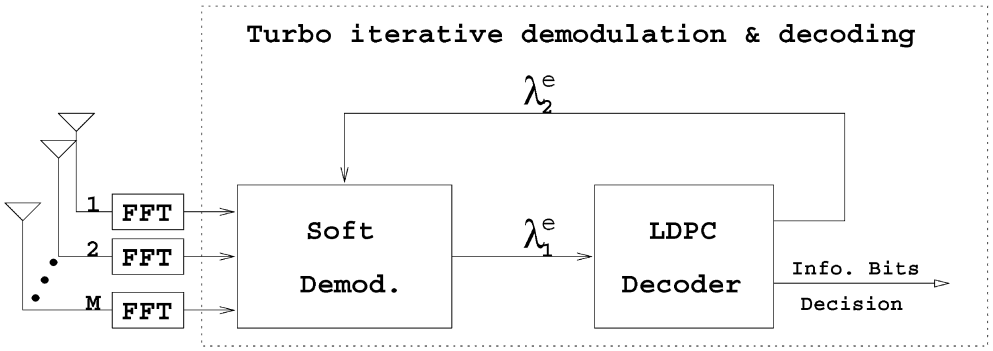

Fig. 3. Turbo receiver structure, which employs a soft demodulator and a soft LDPC decoder, for an LDPC-coded MIMO OFDM system.

III. Iterative Receiver Structure

A serial concatenated turbo iterative receiver is employed (as shown in Fig. 3) to approach the maximum likelihood (ML) receiver performance of joint MIMO OFDM demodulation and LDPC decoding. The extrinsic information of the LDPC-coded bits is iteratively passed between a soft-input-soft-output (abbreviated as "soft") demodulator and a soft belief-propagation LDPC decoder; in each demodulator-decoder iteration, a number of inner iterations is performed within the soft LDPC decoder, during which time, extrinsic information is passed along the edges in the bipartite graph.

In the following, we stick to the following notations. All extrinsic information (message) is in log-likelihood (LLR) form, and the variable L is used to refer to extrinsic information. The variable f is used to denote the probability density function (pdf) of the extrinsic information L, and m is used to denote the mean of L. Superscript (p, q) is used to denote quantities during the pth round of inner decoding within the LDPC decoder and the qth stage of outer iteration between the LDPC decoder and the MIMO OFDM demodulator. For the quantities passed between the soft MIMO OFDM demodulator and the soft LDPC decoder, only one superscript q, namely, the iteration number of turbo iterative receiver, is used. A subscript $D \to L$ denotes quantities passed from the demodulator to the LDPC decoder, and vice versa, $D \leftarrow L$.

A. Demodulation of MIMO OFDM

Assuming the perfect CSI at the receiver, it is clear from (1) that the demodulation of the received signals at a particular subcarrier and a particular slot can be carried out independently. For notational convenience, in this subsection, we temporarily drop the index $[p, k]$.

As illustrated in Fig. 3, at the qth turbo iteration, the soft MIMO OFDM demodulator computes extrinsic information of the LDPC code bit b_i as

$$L^q_{D\to L}(b_i) = g\left(\boldsymbol{y}, \{L^{q-1}_{D\leftarrow L}(b_j)\}_j\right) \tag{6}$$

where $\boldsymbol{y}$ is the received data; $\{L^{q-1}_{D\leftarrow L}(b_j)\}_j$ is the extrinsic information computed by LDPC decoder in the previous turbo iteration at the first turbo iteration $L^{q-1}_{D\leftarrow L}(b_j) \equiv 0, \forall j$; and $g(\cdot)$ denotes the demodulation function, which is described below.

At a given subcarrier and time slot, N symbols or, correspondingly, $N\log_2|\Omega|$ LDPC code bits are transmitted from N transmitter antennas. In a maximum *a posterior* (MAP) MIMO OFDM demodulator, $L^q_{D\to L}(b_i)$ $(i = 1, \ldots, N\log_2|\Omega|)$ is computed as (7), at the bottom of the page, where $\mathcal{C}_i^+$ is the set of $\boldsymbol{x}$ for which the ith LDPC-coded bit is "+1," and $\mathcal{C}_i^-$ is similarly defined; $\{\boldsymbol{x}^+\}_j$ denotes the corresponding jth binary bit in symbol $\boldsymbol{x}^+$, and similarly, so does $\{\boldsymbol{x}^-\}_j$. The soft MAP demodulator in (7) has a complexity at $\mathcal{O}(|\Omega|^N)$ and can

$$\begin{aligned}
L^q_{D\to L}(b_{i,j}) &\triangleq \log\frac{P(b_{i,j}=+1|\boldsymbol{y})}{P(b_{i,j}=-1|\boldsymbol{y})} - \underbrace{\log\frac{P(b_{i,j}=+1)}{P(b_{i,j}=-1)}}_{L^{q-1}_{D\leftarrow L}(b_{i,j})} \\
&= \log\frac{\sum\limits_{\boldsymbol{x}^+\in\mathcal{C}_i^+} P(\boldsymbol{x}=\boldsymbol{x}^+|\boldsymbol{y})}{\sum\limits_{\boldsymbol{x}^-\in\mathcal{C}_i^-} P(\boldsymbol{x}=\boldsymbol{x}^-|\boldsymbol{y})} - L^{q-1}_{D\leftarrow L}(b_{i,j}) \\
&= \log\frac{\sum\limits_{\boldsymbol{x}^+\in\mathcal{C}_i^+} P(\boldsymbol{y}|\boldsymbol{x}=\boldsymbol{x}^+)\,P(\boldsymbol{x}=\boldsymbol{x}^+)}{\sum\limits_{\boldsymbol{x}^-\in\mathcal{C}_i^-} P(\boldsymbol{y}|\boldsymbol{x}=\boldsymbol{x}^-)\,P(\boldsymbol{x}=\boldsymbol{x}^-)} - L^{q-1}_{D\leftarrow L}(b_{i,j}) \\
&= \log\frac{\sum\limits_{\boldsymbol{x}^+\in\mathcal{C}_i^+} \exp\left(-\|\boldsymbol{y}-\sqrt{\frac{\mathrm{SNR}}{N}}\boldsymbol{H}\boldsymbol{x}^+\|^2 + \sum\limits_{j=1}^{N\log_2|\Omega|}\{\boldsymbol{x}^+\}_j\cdot\frac{L^{q-1}_{D\leftarrow L}(b_{k,j})}{2}\right)}{\sum\limits_{\boldsymbol{x}^+\in\mathcal{C}_i^-} \exp\left(-\|\boldsymbol{y}-\sqrt{\frac{\mathrm{SNR}}{N}}\boldsymbol{H}\boldsymbol{x}^-\|^2 + \sum\limits_{j=1}^{N\log_2|\Omega|}\{\boldsymbol{x}^-\}_j\cdot\frac{L^{q-1}_{D\leftarrow L}(b_{k,j})}{2}\right)} - L^{q-1}_{D\leftarrow L}(b_{i,j})
\end{aligned} \tag{7}$$

only be used in practice for small constellation size and small number of transmit antennas.

We next describe a suboptimal soft demodulator, which is based on the linear minimum-mean-square-error soft-interference-cancellation (LMMSE-SIC) techniques [18] and has a relatively low complexity at $\mathcal{O}(|\Omega|^3)$.

Based on the *a priori* LLR of the code bits provided by the LDPC decoder $\{L^{q-1}_{D\leftarrow L}(b_i)\}_i$, we first form soft estimates of the symbol transmitted from the jth $(j=1,2,\ldots,N)$ antenna as

$$\begin{aligned}\tilde{x}_j &\triangleq \sum_{\hat{x}\in\Omega}\hat{x}P\left(x_j=\hat{x}\right)\\ &= \sum_{\hat{x}\in\Omega}\hat{x}\prod_{l=1}^{\log_2|\Omega|}\left[1+\exp\left(-\{\hat{x}\}_l\cdot L^{q-1}_{D\leftarrow L}(b_{l,j})\right)\right]^{-1} \quad (8)\end{aligned}$$

where $b_{l,j}$ denotes the correspoding lth binary bit in symbol x_j. Denote

$$\tilde{\boldsymbol{x}}_j \triangleq \left[\tilde{x}_1,\ldots,\tilde{x}_{j-1},0,\tilde{x}_{j+1},\ldots,\tilde{x}_{N-1}\right]^T. \quad (9)$$

We then perform a soft interference cancellation $\boldsymbol{y}_j$ to obtain

$$\tilde{\boldsymbol{y}}_j \triangleq \boldsymbol{y}-\boldsymbol{H}\tilde{\boldsymbol{x}}_j = \boldsymbol{H}\left(\boldsymbol{x}-\tilde{\boldsymbol{x}}_j\right)+\boldsymbol{n}. \quad (10)$$

Next, an instantaneous linear MMSE filter is applied to $\tilde{\boldsymbol{y}}_j$ to obtain

$$z_j = \boldsymbol{w}_j^H\tilde{\boldsymbol{y}}_j \quad (11)$$

where the filter $\boldsymbol{w}_j \in \mathcal{C}^M$ is chosen to minimize the mean-square error between the transmit symbol x_j and the filter output z_j, i.e.,

$$\begin{aligned}\boldsymbol{w}_j &= \arg\min_{\boldsymbol{w}\in\mathcal{C}^M} E\left\{|x_j-\boldsymbol{w}^H\tilde{\boldsymbol{y}}_j|^2\right\}\\ &= \sqrt{\frac{N}{\mathrm{SNR}}}\left(\boldsymbol{H}\boldsymbol{\Delta}_j\boldsymbol{H}^H+\frac{N}{\mathrm{SNR}}\boldsymbol{I}\right)^{-1}\boldsymbol{H}\boldsymbol{e} \quad (12)\end{aligned}$$

where

$$\begin{aligned}\boldsymbol{\Delta}_j &\triangleq \mathrm{cov}\{\boldsymbol{x}_j-\tilde{\boldsymbol{x}}_j\}\\ &= \mathrm{diag}\left\{1-|\tilde{x}_1|^2,\ldots,1-|\tilde{x}_{j-1}|^2,1,1\right.\\ &\qquad \left.-|\tilde{x}_{j+1}|^2,\ldots,1-|\tilde{x}_N|^2\right\} \quad (13)\end{aligned}$$

and $\boldsymbol{e}$ denotes an M-sized vector with all-zero entries, except for the jth entry being 1. The detailed derivation of (12) is further referred to [18].

As in [18], we approximate the soft instantaneous MMSE filter output z_j in (11) as Gaussian distributed, i.e.,

$$p(z_j \mid x_j) \sim \mathcal{N}_c\left(\mu_j x_j, \eta_j^2\right). \quad (14)$$

Conditioned on x_j, the mean and variance of z_j are given, respectively, by

$$\begin{aligned}\mu_j &\triangleq E\{z_j x_j^*\}\\ &= \boldsymbol{e}^T\boldsymbol{H}^H\left(\boldsymbol{H}\boldsymbol{\Delta}_j\boldsymbol{H}^H+\frac{N}{\mathrm{SNR}}\boldsymbol{I}\right)^{-1}\boldsymbol{H}\boldsymbol{e} \quad (15)\\ \eta_j^2 &\triangleq \mathrm{var}\{z_j\}\\ &= E\{|z_j|^2\}-\mu_j^2 = \mu_j-\mu_j^2. \quad (16)\end{aligned}$$

The extrinsic information $L^q_{D\to L}(b_{i,j})$ of the corresponding ith binary bit in symbol x_j delivered by the LMMSE-SIC demodulator is calculated as (17), shown at the bottom of the page, where $\mathcal{S}^+_{i,j}$ is the set of all possible values of x_i for which the ith LDPC-coded bit is "+1," and $\mathcal{S}^-_{i,j}$ is similarly defined; $\{x_j^+\}_k$ denotes the corresponding kth binary bit in symbol x_j^+, and similarly, so does $\{x_j^-\}_k$. Note that the LMMSE-SIC demodulator extracts the extrinsic LLR of code bit b_i from z_j, which is the *scalar* output of the LMMSE filter in (11), whereas the MAP demodulator collects the extrinsic LLR from $\boldsymbol{y}$, which is the M-size *vector* of the received signals. The complexity of soft LMMSE-SIC demodulator, hence, is significantly lower than that of the soft MAP demodulator, especially when N and $|\Omega|$ are large.

B. Decoding of LDPC Codes

The message-passing (also known as belief-propagation) decoding algorithm is used to decode the LDPC codes [14]. To describe the message-passing decoding algorithm, the following notations are first introduced. In the bipartite graph of the LDPC codes, the variable (bit) nodes are numbered

$$\begin{aligned}L^q_{D\to L}(b_i) &\triangleq \log\frac{P\left(b_i=+1|z_j\right)}{P\left(b_i=-1|z_j\right)} - \underbrace{\log\frac{P\left(b_i=+1\right)}{P\left(b_i=-1\right)}}_{L^{q-1}_{D\leftarrow L}(b_i)}\\ &= \log\frac{\sum_{x^+\in\mathcal{S}^+_{i,j}}P\left(x_j=x^+|z_j\right)}{\sum_{x^-\in\mathcal{S}^-_{i,j}}P\left(x_j=x^-|z_j\right)} - L^{q-1}_{D\leftarrow L}(b_i)\\ &= \log\frac{\sum_{x^+\in\mathcal{S}^+_{i,j}}P\left(z_j|x_j=x^+\right)P\left(x_j=x^+\right)}{\sum_{x^-\in\mathcal{S}^-_{i,j}}P\left(z_j|x_j=x^-\right)P\left(x_j=x^-\right)} - L^{q-1}_{D\leftarrow L}(b_i)\\ &= \log\frac{\sum_{x^+\in\mathcal{S}^+_{i,j}}\exp\left(\frac{-\|z_j-\mu_j x^+\|^2}{\eta_j^2}+\sum_{k=1}^{\log_2|\Omega|}\{x_j^+\}_k\cdot\frac{L^{q-1}_{D\leftarrow L}(b_k)}{2}\right)}{\sum_{x_j^+\in\mathcal{S}^-_{i,j}}\exp\left(\frac{-\|z_j-\mu_j x^-\|^2}{\eta_j^2}+\sum_{k=1}^{\log_2|\Omega|}\{x_j^-\}_k\cdot\frac{L^{q-1}_{D\leftarrow L}(b_k)}{2}\right)} - L^{q-1}_{D\leftarrow L}(b_i) \quad (17)\end{aligned}$$

from 1 to n, the check nodes from 1 to $n-k$ (in any order). The degree of the ith variable node is denoted by ν_i, and the degree of the ith check node is denoted by Δ_i. Denote by $\{e^b_{i,1}, e^b_{i,2}, \ldots, e^b_{i,\nu_i}\}$ the set of edges connected to the ith variable node and by $\{e^c_{i,1}, e^c_{i,2}, \ldots, e^c_{i,\Delta_i}\}$ the set of edges connected to the ith check node. That is, $e^b_{i,k}$ denotes the kth edge connected to the ith variable node, and $e^c_{i,k}$ denotes the kth edge connected to the ith check node. The particular edge or bit associated with an extrinsic message is denoted as the argument of L. A subscript $b \to c$ denotes quantities passed from the variable nodes to the check nodes of the LDPC code, and vice versa. For example, $L^{p,q}_{b\to c}(e^b_{i,j})$ denotes the extrinsic LLR passed from a variable node to a check node along the jth edge connected to the ith variable node, during the pth iteration within the LDPC decoder and the qth iteration between the LDPC decoder and the demodulator. For the pdf's f and means m, no argument is used since they do not depend on the particular edge, variable node, or check node.

The message-passing decoding algorithm of LDPC codes is summarized as follows.

- *Iterate between variable node update and check node update*: For $p = 1, 2, \ldots, P$.

— *Variable node update*: For each of the variable nodes $i = 1, 2, \ldots, n$, for every edge connected to the variable node, compute the extrinsic message passed from the variable node to the check node along the edge, given by

$$L^{p,q}_{b\to c}(e^b_{i,j}) = L^q_{D\to L}(b_i) + \sum_{k=1,k\neq j}^{\nu_i} L^{p-1,q}_{b\leftarrow c}(e^b_{i,k}). \tag{18}$$

— *Check node update*: For each of the check nodes $i = 1, 2, \ldots, n-k$, for all edges that are connected to the check node, compute the extrinsic message passed from the check node to the variable node, given by [19]

$$L^{p,q}_{b\leftarrow c}(e^c_{i,j}) = 2\tanh^{-1}\left[\prod_{k=1,k\neq j}^{\Delta_i} \tanh\left(\frac{L^{p,q}_{b\to c}(e^c_{i,k})}{2}\right)\right]. \tag{19}$$

- *Compute extrinsic messages passed back to the demodulator*:

$$L^q_{D\leftarrow L}(b_i) = \sum_{k=1}^{\nu_i} L^{P,q}_{b\leftarrow c}(e^b_{i,k}). \tag{20}$$

- *Store check node to variable node messages*: For all edges, set

$$L^{0,q+1}_{b\leftarrow c}(e^b_{i,k}) = L^{P,q}_{b\leftarrow c}(e^b_{i,k}). \tag{21}$$

After sufficient Q times turbo receiver iterations, final hard decisions on information and parity bits are made as

$$\hat{b}_i = \operatorname{sign}\left[L^Q_{D\to L}(b_i) + L^Q_{D\leftarrow L}(b_i)\right]. \tag{22}$$

IV. Analysis and Optimization of LDPC-Coded MIMO OFDM

In this section, we describe how to analyze and optimize the LDPC-coded MIMO OFDM systems via the techniques of density evolution with mixture Gaussian approximations [15]. The principal idea of density evolution [12]–[14] is to treat the extrinsic information that is passed in the iterative process as random variables. Then, by estimating the pdf of the random variables as a function of SNR and iteration number, we can compute the probability of error at every iteration. When the length of the codewords $n \to \infty$, the extrinsic information passed along the edges connected to every check node and variable node can be assumed to be independent variables. This makes it possible to compute the pdfs relatively easily. The minimum SNR for which the probability of error tends to zero is called the minimum operational SNR, which is denoted by $\mathrm{SNR}_{\min\_op}$.

A. Mixture Gaussian Approximation to the Distribution of Extrinsic Messages

It is known that the extrinsic information passed from soft LDPC decoder to soft MIMO OFDM demodulator $f^q_{D\leftarrow L}$ can be modeled as mixture symmetric Gaussian distributed [12], [20], [21]. A mathematical expression of $f^q_{D\leftarrow L}$ can be referred to (43). We remark that such a mixture Gaussian model is due to the code structure and the belief-propagation decoding algorithm of LDPC codes.

On the other hand, the pdf of the extrinsic information passed from soft MIMO OFDM demodulator to soft LDPC decoder $f^q_{D\to L}$ in general has no closed-form expression. Next, we propose to approximate it as a mixture of symmetric Gaussians. That is, we model the pdf of the soft demodulator output LLR as

$$f^q_{D\to L} \cong \sum_{j=1}^{J} \pi_j \mathcal{N}(m_j, 2m_j). \tag{23}$$

In particular, we are interested in approximating the exact pdf in (23) with finite J terms. For a fixed number of mixtures J, based on the observations $\Xi \triangleq \{\xi_i, i = 1, \ldots, n\}$, the parameters $\boldsymbol{\theta} \triangleq \{\pi_j, m_j, j = 1, \ldots, J\}$ can be estimated using the expectation-maximization (EM) algorithm, which is explained next.

Denote $\phi(x; \mu, \sigma^2)$ as the pdf of an $\mathcal{N}(\mu, \sigma^2)$ random variable. Then, the maximum likelihood (ML) estimate of the parameters $\boldsymbol{\theta}$ is given by

$$\begin{aligned}\hat{\boldsymbol{\theta}} &= \arg \max_{\boldsymbol{\theta}:\sum_{j=1}^{J}\pi_j=1} \log p_{\boldsymbol{\theta}}(\Xi) \\ &= \arg \max_{\boldsymbol{\theta}:\sum_{j=1}^{J}\pi_j=1} \sum_{i=1}^{n} \log \sum_{j=1}^{J} \pi_j \phi(\xi_i; m_j, 2m_j). \end{aligned} \tag{24}$$

Direct solution to the above maximization problem is very difficult. The EM algorithm [22], [23] is an iterative procedure for solving this ML estimation problem.

In the EM algorithm, the observation Ξ is termed as *incomplete* data. Starting from some initial estimate $\boldsymbol{\theta}^{(0)}$, the EM algorithm solves the ML estimation problem (24) by the following iterative procedure:

- E-step: Compute

$$Q(\boldsymbol{\theta} \mid \boldsymbol{\theta}^{(i)}) = E_{\boldsymbol{\theta}^{(i)}}\left\{\log p_{\boldsymbol{\theta}}(\boldsymbol{X}) \mid \Xi\right\}. \tag{25}$$

- M-step: Solve

$$\boldsymbol{\theta}^{(i+1)} = \arg\max_{\boldsymbol{\theta}} Q\left(\boldsymbol{\theta} \mid \boldsymbol{\theta}^{(i)}\right). \tag{26}$$

Define the following hidden data $\boldsymbol{Z} = \{\boldsymbol{z}_i, i = 1, \ldots, n\}$, where $\boldsymbol{z}_i$ is a J-dimensional indicator vector such that

$$z_{i,j} = \begin{cases} 1, & \text{if } \xi_i \sim \mathcal{N}(m_j, 2m_j) \\ 0, & \text{otherwise.} \end{cases} \tag{27}$$

The complete data is then $\boldsymbol{X} \triangleq (\Xi, \boldsymbol{Z})$. We have

$$p_{\boldsymbol{\theta}}(\Xi, \boldsymbol{Z}) = \prod_{i=1}^{n} \prod_{j=1}^{J} [\pi_j \phi(\xi_i; m_j, 2m_j)]^{z_{i,j}}. \tag{28}$$

The log-likelihood function of the complete data is then given by

$$\log p_{\boldsymbol{\theta}}(\Xi, \boldsymbol{Z}) = \sum_{i=1}^{n} \sum_{j=1}^{J} z_{i,j} \log \pi_j + \sum_{i=1}^{n} \sum_{j=1}^{J} z_{i,j} \left[-\frac{1}{2} \log 2m_j - \frac{(\xi_i - m_j)^2}{4m_j} \right] + C \tag{29}$$

where C is some constant. The E-step can then be calculated as follows:

$$\begin{aligned} Q(\boldsymbol{\theta}, \boldsymbol{\theta}') &= E'_{\boldsymbol{\theta}} \{ \log p_{\boldsymbol{\theta_O}}(\Xi, \boldsymbol{Z}) \mid \Xi \} \\ &= \sum_{i=1}^{n} \sum_{j=1}^{J} \hat{z}_{i,j} \left[\log \pi_j - \frac{1}{2} \log 2m_j - \frac{(\xi_i - m_j)^2}{4m_j} \right] + C, \end{aligned} \tag{30}$$

where

$$\begin{aligned} \hat{z}_{i,j} &= E'_{\boldsymbol{\theta}} \{ z_{i,j} \mid \Xi, \boldsymbol{\theta}' \} = P'_{\boldsymbol{\theta}} \{ z_{i,j} = 1 \mid \xi_i \} \\ &= \frac{p'_{\boldsymbol{\theta}}(\xi_i \mid z_{i,j} = 1) P'_{\boldsymbol{\theta}}(z_{i,j} = 1)}{\sum_{l=1}^{J} p'_{\boldsymbol{\theta}}(\xi_i \mid z_{i,l} = 1) P'_{\boldsymbol{\theta}}(z_{i,l} = 1)} \\ &= \frac{\phi(\xi_i; m'_j, 2m'_j)\pi'_j}{\sum_{l=1}^{J} \phi(\xi_i; m'_l, 2m'_l)\pi'_l}. \end{aligned} \tag{31}$$

In addition, the M-step is calculated as follows. To obtain $\{\pi_j\}$, we have

$$\frac{\partial Q(\boldsymbol{\theta}, \boldsymbol{\theta}')}{\partial \pi_j} = 0 \Rightarrow \pi_j = \frac{1}{n} \sum_{i=1}^{n} \hat{z}_{i,j}, \quad j = 1, \ldots, J. \tag{32}$$

To obtain $\{m_j\}$, we have

$$\begin{aligned} \frac{\partial Q(\boldsymbol{\theta}, \boldsymbol{\theta}')}{\partial m_j} = 0 &\Rightarrow m_j^2 + 2m_j - \frac{\sum_{i=1}^{n} \hat{z}_{i,j} \xi_i^2}{\sum_{i=1}^{n} \hat{z}_{i,j}} = 0 \\ &\Rightarrow m_j = -1 + \sqrt{1 + \frac{\sum_{i=1}^{n} \hat{z}_{i,j} \xi_i^2}{\sum_{i=1}^{n} \hat{z}_{i,j}}} \\ &j = 1, \ldots, J. \end{aligned} \tag{33}$$

Finally, the EM algorithm for calculating the Gaussian mixture parameters for the extrinsic messages passed from the demodulator is summarized as follows.

- *Given the demodulator extrinsic messages* $\{\xi_i\}$, *the number of mixture components* J, *and the total number of EM iterations* I, *starting from the initial parameters* $\boldsymbol{\theta}^{(0)}$: For $i = 1, \ldots, I$, do the following.
  - Let $\boldsymbol{\theta}' = \boldsymbol{\theta}^{(i-1)}$, and calculate $\{\hat{z}_{i,j}, i = 1, \ldots, n; j = 1, \ldots, J\}$ according to (31).
  - Calculate $\{\pi_j, j = 1, \ldots, J\}$ according to (32), and calculate $\{m_j, j = 1, \ldots, J\}$ according to (33). Set $\boldsymbol{\theta}^{(i)} = \boldsymbol{\theta}$.

In the above EM algorithm, the number of mixture components J is fixed. Note that when J increases, $\log p_{\boldsymbol{\theta}}(\Xi)$ increases, or $-\log p_{\boldsymbol{\theta}}(\Xi)$ decreases. The minimum description length (MDL) principle can be used to determine J [24], [25],

$$\hat{J}_{MDL} = \arg \min_{J} \left\{ -\log p_{\boldsymbol{\theta}, J}(\Xi) + \frac{J}{2} \log n \right\} \tag{34}$$

where, in the MDL criterion, a penalty term $J/2 \log n$ is introduced. Hence, we can first set an upper bound of the number of mixture components, $J_{\max}$. In addition, for each $J \leq J_{\max}$, we run the above EM algorithm and calculate the corresponding MDL value. Finally, we choose the optimal J with the minimum MDL.

B. Density Evolution With Gaussian Approximation

In [12], it was assumed that the extrinsic messages at the output of each variable or check node is Gaussian and symmetric (i.e., the variance is twice the mean). Therefore, the pdf of the extrinsic messages at the output of each variable or check node is entirely characterized by its mean. Only the AWGN channel was considered in [12], and since the pdf at the channel output is Gaussian for the AWGN channel, this characterization was accurate. Here, we will treat the more general case where the pdf at the demodulator output is a mixture of symmetric Gaussians and derive the steps involved in computing the pdfs of the extrinsic LLRs at each iteration. We will show that due to the assumption that the demodulator output is a mixture of symmetric Gaussian pdfs, we can easily track the pdfs of the extrinsic LLRs within the LDPC code without having to numerically convolve or evaluate pdfs. This significantly reduces the complexity in code design without sacrificing much performance. Similar to [12], we assume that $f_{b \leftarrow c}^{p,q}$ is Gaussian at each check node. Note that due to the irregularity of the LDPC codes, this assumption means that the pdfs of the extrinsic LLRs are all mixtures of symmetric Gaussian pdfs. We only have to evaluate the means of the component Gaussian pdfs in order to track the pdf.

We next specify the procedure for computing the pdfs of the extrinsic messages passed around in the turbo iterative receiver algorithm described in Section III. Denoting $\psi(x) \triangleq E\{\tanh[1/2\mathcal{N}(x, 2x)]\}$, we get the following.

- *Initialization*: Set $f_{b \leftarrow c}^{0,0}(x) = \delta(x)$, and $f_{D \leftarrow L}^{0}(x) = \delta(x)$.
- *Turbo iterative iterations*: For $q = 1, 2, \ldots, Q$, do the following.
  - *Compute the pdf of extrinsic messages passing from the demodulator*: $f_{D \rightarrow L}^{q}$ is computed as a function of SNR and $f_{D \leftarrow L}^{q-1}$ using the method in Section IV-A to obtain

$$f_{D \rightarrow L}^{q} = \sum_{j=1}^{J} \pi_j \mathcal{N}(\mu_j, 2\mu_j). \tag{35}$$

— *Compute the pdf of the LDPC extrinsic messages:*

- *Iterate between variable node update and check node update*: For $p = 1, 2, \ldots, P$, do the following.
  - *At a variable node of degree i*: From (18), we can see that the pdf of the extrinsic LLR that is passed along an edge connected to a variable node of degree i, which is denoted by $f^{p,q}_{b\to c,i}$, is the convolution of $f^{q}_{D\to L}$ with $(i-1)$ convolutions of the pdf $f^{p-1,q}_{b\leftarrow c}$ with itself. We can simplify this by making the assumption that the output extrinsic from the variable node of degree i excluding the contribution from the channel is Gaussian. The same assumption has been made in [12]. That is

$$\begin{aligned} f^{p,q}_{b\to c,i} &= f^{q}_{D\to L} \otimes \mathcal{N}\left((i-1)m^{p-1,q}_{b\leftarrow c}, 2(i-1)m^{p-1,q}_{b\leftarrow c}\right) \\ &= \left(\sum_{j=1}^{J} \pi_j \mathcal{N}(\mu_j, 2\mu_j)\right) \\ &\quad \otimes \mathcal{N}\left((i-1)m^{p-1,q}_{b\leftarrow c}, 2(i-1)m^{p-1,q}_{b\leftarrow c}\right) \\ &= \sum_{j=1}^{J} \pi_j \mathcal{N}\Big(\mu_j + (i-1)m^{p-1,q}_{b\leftarrow c} \\ &\qquad 2\left[\mu_j + (i-1)m^{p-1,q}_{b\leftarrow c}\right]\Big). \end{aligned} \tag{36}$$

  Since λ_i fractions of the edges are connected to variable nodes of degree i, the pdf of the extrinsic message passed from the variable nodes to the check nodes along an edge is

$$\begin{aligned} f^{p,q}_{b\to c} &= \sum_{j=2}^{d_{l,\max}} \lambda_i f^{p,q}_{b\to c,i} \\ &= \sum_{j=1}^{J} \sum_{i=2}^{d_{l,\max}} \pi_j \lambda_i \mathcal{N}\Big(\mu_j + (i-1)m^{p-1,q}_{b\leftarrow c} \\ &\qquad 2\left[\mu_j + (i-1)m^{p-1,q}_{b\leftarrow c}\right]\Big). \end{aligned} \tag{37}$$

  - *At check node of degree j*: Assume that the ith check node is of degree j and that the extrinsic LLR at the output of this check node is Gaussian with mean $m^{p,q}_{b\leftarrow c,j}$. To compute $m^{p,q}_{b\leftarrow c,j}$, we take the expectation on both sides of (19) and get

$$\begin{aligned} & E\left\{\tanh\left(\frac{L^{p,q}_{b\leftarrow c}(e^{c}_{i,r})}{2}\right)\right\} \\ &= E\left\{\left[\prod_{k=1,k\neq r}^{j} \tanh\left(\frac{L^{p,q}_{b\to c}(e^{c}_{i,k})}{2}\right)\right]\right\} \\ &= \left[E\left\{\tanh\left(\frac{L^{p,q}_{b\to c}(e^{c}_{i,k})}{2}\right)\right\}\right]^{j-1} \end{aligned} \tag{38}$$

  where (38) follows from the fact that $L^{p,q}_{b\to c}(e^{c}_{i,k})$ and $L^{p,q}_{b\to c}(e^{c}_{i,s})$ are identically distributed and are independent for $k \neq s$. Since the distribution of $L^{p,q}_{b\leftarrow c}(e^{c}_{i,r})$ will be same for all r (i.e., the message passed along all the edges connected to a check node have the same distribution), we can drop r. Using the distribution of $L^{p,q}_{b\to c}(e^{c}_{i,k})$ given in (37) and the definition of the function $\psi(\cdot)$, we get

$$\psi(m^{p,q}_{b\leftarrow c,j}) = \left(\sum_{l=1}^{J}\sum_{i=2}^{d_{l,\max}} \pi_j \lambda_i \psi(m^{p,q}_{b\to c,i})\right)^{j-1} \tag{39}$$

  where $m^{p,q}_{b\leftarrow c,j}$ is the mean of the LLR passed along an edge at the output of a check node of degree j. Therefore

$$m^{p,q}_{b\leftarrow c,j} = \psi^{-1}\left[\left(\sum_{l=1}^{J}\sum_{i=2}^{d_{l,\max}} \pi_l \lambda_i \psi\left(m^{p,q}_{b\to c,i}\right)\right)^{j-1}\right]. \tag{40}$$

  Since ρ_j fractions of the edges are connected to checks of degree j, the pdf of the extrinsic message passed from the check node to variable node is

$$f^{p,q}_{b\leftarrow c} = \sum_{j=2}^{d_{r,\max}} \rho_j \mathcal{N}\left(m^{p,q}_{b\leftarrow c,j}, 2m^{p,q}_{b\leftarrow c,j}\right). \tag{41}$$

  - *Message passed back to the demodulator*: At variable node of degree i, by taking expectation on both sides of (20), we get

$$m^{q}_{D\leftarrow L}(i) = i m^{p-1,q}_{b\leftarrow c}. \tag{42}$$

  Since a fraction $\tilde{\lambda}_i$ of the *nodes* have degree i

$$f^{q}_{D\leftarrow L} = \sum_{i=2}^{d_{l,\max}} \tilde{\lambda}_i \mathcal{N}\left(m^{q}_{D\leftarrow L}(i), 2m^{q}_{D\leftarrow L}(i)\right). \tag{43}$$

- The $\text{SNR}_{\min .op}$ can be computed as the minimum SNR for which the mean $m^{Q}_{D\leftarrow L}$ or $m^{P,Q}_{b\leftarrow c}$ tends to ∞. That is

$$\text{SNR}_{\min .op} \triangleq \min \text{SNR} : \lim_{n\to\infty} \lim_{\substack{P\to\infty \\ Q\to\infty}} m^{P,Q}_{b\leftarrow c} \to \infty. \tag{44}$$

The procedure for computing the $\text{SNR}_{\min .op}$ for a given degree profile $(\lambda(x), \rho(x))$ can be used in conjunction with an optimization procedure to design optimal LDPC-coded MIMO OFDM systems. The idea is to find optimal $\lambda(x)$ and $\rho(x)$ such that the $\text{SNR}_{min.op}$ is minimized. Note that the rate of the LDPC code is $r = 1 - \int_0^1 \rho(x)\,dx / \int_0^1 \lambda(x)\,dx$. A nonlinear optimization procedure called differential evolution [26], [27] is employed here to solve the above optimization problem.

V. Numerical Results

In this section, we present numerical results for the design and optimization of LDPC-coded MIMO OFDM systems. For each transmit-receive-antenna pair, DoCoMo's physical fading channel model, exponentially distributed frequency-selective fading with 88.8 ns maximum delay spread, is adopted. OFDM modulation is used with subcarrier spacing 131.836 kHz and cyclic prefix interval of 1.54 μs; as a parameter to be discussed, the number of subcarriers K is specified next. It is clear that the total bandwidth is approximately K times of the subcarrier

spacing, and the multipath resolution of the frequency-selective fading channel is the inverse of total bandwidth. For instance, with $K = 1024$, there are 12 resolvable paths in DoCoMo's channel model, but with $K = 512$, the number of resolvable paths is reduced to 6. The modulator uses the quadrature phase shift keying (QPSK) constellation with Gray mapping; for the considered MIMO systems with large number of antennas, the capacity (both ergodic and outage) difference between QPSK signaling and Gaussian signaling is small (e.g., ~ 0.2 dB at 4 bits/Hz/s when $N = M = 4$). All the LDPC codes designed and optimized below have rate 1/2 and appropriate code lengths. For clarity, the rate loss due to cyclic prefix is not counted in this paper.

All the regular LDPC codes are ($s = 3$, $t = 6$) codes taken from [28]. All the irregular LDPC codes are obtained from the design procedure proposed in this paper. For example, the optimized degree profile for the spatially uncorrelated 2×2 MIMO OFDM systems employing the MAP demodulator is $\lambda(x) = 0.269\,052x + 0.135\,031x^2 + 0.024\,564x^4 + 0.028\,685x^5 + 0.075\,819x^6 + 0.033\,661x^7 + 0.024\,360x^8 + 0.020\,951x^9 + 0.018\,975x^{10} + 0.014\,373x^{12} + 0.035\,585x^{13} + 0.015\,569x^{14} + 0.013\,611x^{16} + 0.289\,765x^{19}$ and $\rho(x) = 0.307\,710x^7 + 0.692\,290x^8$, and that for the spatially uncorrelated 2×2 MIMO OFDM systems employing the LMMSE-SIC demodulator is $\lambda(x) = 0.294\,388x + 0.100\,255x^2 + 0.056\,131x^3 + 0.042\,069x^4 + 0.032\,675x^5 + 0.065\,028x^7 + 0.030\,813x^8 + 0.027\,357x^9 + 0.025\,533x^{10} + 0.029\,996x^{11} + 0.014\,911x^{15} + 0.020\,255x^{17} + 0.013\,650x^{18} + 0.246\,939x^{19}$ and $\rho(x) = 0.738\,497x^7 + 0.261\,503x^8$.

In Sections V-A–C, the performance of the LDPC codes in ergodic MIMO OFDM channels is demonstrated by bit-error-rate (BER) versus SNR [see (2)]; in Section V-D, the performance in outage MIMO OFDM channels is demonstrated by frame-error-rate (FER) versus SNR.

A. Different Number of Antennas

If only single-transmit-receive-antenna is used, a cellular system designed for 100 Mb/s peak rate downlink transmission requires very broad spectrum, as well as broadband transceiver circuitry; either of which could be costly for commercial applications. MIMO techniques provide a promising means to ameliorate this issue. For example, to achieve a fixed data rate of 100 Mb/s, a traditional single-antenna system requires 100 MHz bandwidth (assume QPSK modulation and coding rate 1/2), whereas a four-transmit, four-receive antenna system could potentially transmit the same 100 Mb/s data rate using only 25 MHz bandwidth. We note that the information rate in the single-antenna system is 1 bit/Hz/s, whereas in the 4×4 MIMO system, it is increased to 4 bits/Hz/s (higher information rate indicates a more efficient use of spectral resource).

In our study, it is assumed that the number of receive antennas is the same as the number of transmit antennas, i.e., $N = M$. We consider 1×1, 2×2 and 4×4 MIMO OFDM systems. Without spatial correlation, $\boldsymbol{R}_l = \boldsymbol{S}_l = \boldsymbol{I}$ in (1) (the systems with spatial correlation will be discussed in Section V-C). The design and optimization results are shown in Figs. 4–6. In these

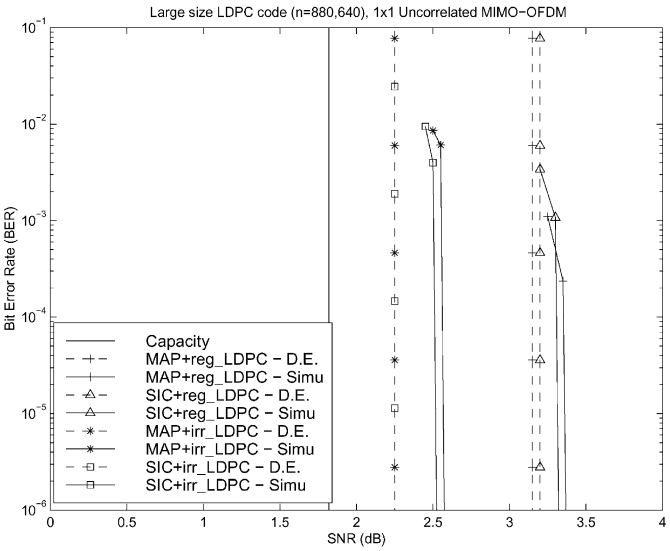

Fig. 4. Performance computed by density evolution analysis and computer simulations for ergodic 1×1 MIMO OFDM channels with no spatial correlation.

figures, the ergodic channel capacity computed from (3) and (5) is denoted by "Capacity." First, we focus on the performance of iterative receiver employing soft MAP demodulator, i.e., the curves denoted by "MAP + regLDPC − D.E.," "MAP + regLDPC − Simu," "MAP + irrLDPC − D.E.," and "MAP + irrLDPC − Simu," where the suffix "D.E." denotes the results from density evolution analysis, and "Simu" denotes that from computer simulations. In order to achieve ergodic channel capacity, large block-size LDPC codes ($n = 880\,640$) are used to capture large number of fading channel realizations ($\tilde{n} = 430$). It is seen that by applying MIMO techniques, the information rate is increased to N bits/Hz/s, whereas the ergodic capacity (the "Capacity" curve) is also slightly improved. Moreover, by employing the optimized irregular LDPC codes and the turbo iterative receiver employing the MAP demodulator, the operational $\text{SNR}_{min.op}$ of LDPC-coded MIMO OFDM systems is within 1 dB from the information theoretic ergodic capacity. It is also seen that the performance calculated by density evolution analysis (the "D.E." curves) matches that obtained from simulations (the "Simu" curves). Finally, we observe that the performance gap between the regular and the irregular LDPC codes tends to be smaller for systems with a larger number of antennas.

B. Different Demodulation Schemes

The performance when employing suboptimal LMMSE-SIC demodulator is demonstrated in Figs. 4–6 by the curves "SIC + regLDPC − D.E.," "SIC + regLDPC − Simu," "SIC + irrLDPC − D.E.," and "SIC + irrLDPC − Simu." Compared with the MAP demodulator-based performance (as in Section V-A), the use of the LMMSE-SIC demodulator brings less than 1 dB performance loss for 1×1, 2×2, and 4×4 systems. Therefore, in spatially uncorrelated ergodic MIMO OFDM channels, the LMMSE-SIC demodulator appears to be a promising choice in practical implementation for its good performance and relatively low complexity.

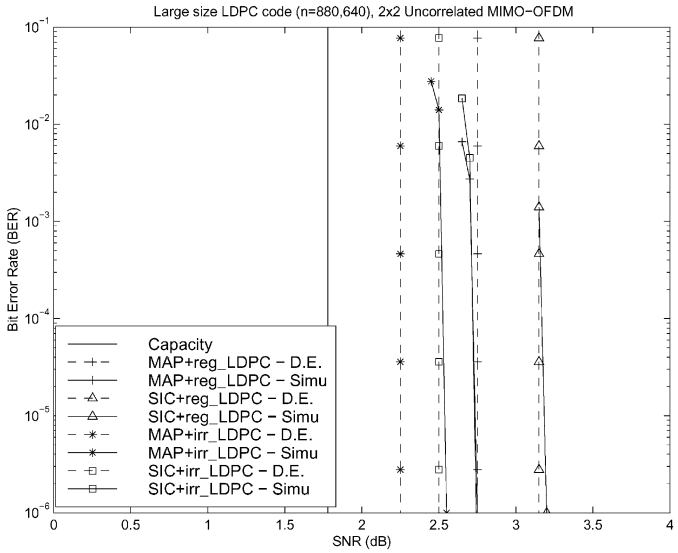

Fig. 5. Performance computed by density evolution analysis and computer simulations for ergodic 2×2 MIMO OFDM channels with no spatial correlation.

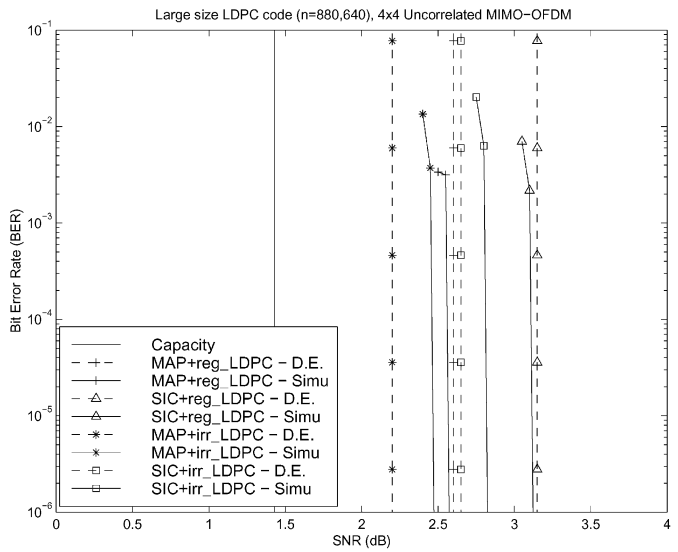

Fig. 6. Performance computed by density evolution analysis and computer simulations for ergodic 4×4 MIMO OFDM channels with no spatial correlation.

C. Spatial Correlation

In this subsection, we discuss the performance of MIMO OFDM systems with spatial (antenna) correlation. Following [16], we assume uniform linear antenna placement at both the transmitter and the receiver. The antenna correlation matrices $\boldsymbol{R}_l$ and $\boldsymbol{S}_l$ are given by

$$[\boldsymbol{R}_l]_{m,n} = \exp\left[-j2\pi(n-m)d_T\cos(\bar{\theta}_{T,l}) \right. \\ \left. \frac{-(2\pi(n-m)d_T\sin(\bar{\theta}_{T,l})\sigma_{\theta_{T,l}})^2}{2}\right] \quad (45)$$

$$[\boldsymbol{S}_l]_{m,n} = \exp\left[-j2\pi(n-m)d_R\cos(\bar{\theta}_{R,l}) \right. \\ \left. \frac{-(2\pi(n-m)d_R\sin(\bar{\theta}_{R,l})\sigma_{\theta_{R,l}})^2}{2}\right] \quad (46)$$

where $[\boldsymbol{A}]_{m,n}$ denotes the (m,n)th element of matrix $\boldsymbol{A}$; d_T denotes the transmitter antenna spacing normalized by carrier wavelength; $\bar{\theta}_{T,l}$ denotes the mean angle of departure for each scatterer cluster at the transmitter; $\sigma_{\theta_{T,l}}$ denotes the root-mean-square (RMS) of angle of departure at the transmitter; and d_R, $\bar{\theta}_{R,l}$, and $\sigma_{\theta_{R,l}}$ denote the corresponding variables at the receiver side. In our experiments, we consider an urban micro-cell scenario [29] and, for simplicity, assume that all L paths follow the same spatial parameters as $\bar{\theta}_{T,l} = 53, \bar{\theta}_{R,l} = 18$, $\sigma_{\theta_{T,l}} = 8$, and $\sigma_{\theta_{R,l}} = 2$; we also let $d_T = 4.0$ and $d_R = 0.5$ to reflect the situations that the antennas at base station are easier to sparsely place than the antennas at mobile devices. It is worth noting that some parameters (e.g., $\sigma_{\theta_{R,l}} = 2$) here are intentionally set to be worse than typical scenarios in order to highlight the effect of spatial correlation. Going through the same design and optimization procedure, we obtain the analysis and design results in Figs. 7 and 8. (The issue of antenna correlation does not exist for 1×1 systems.) Compared with spatially uncorrelated systems, antenna correlation causes channel capacity loss for the systems considered here. Nevertheless, the optimized irregular LDPC codes along with the MAP demodulator-based

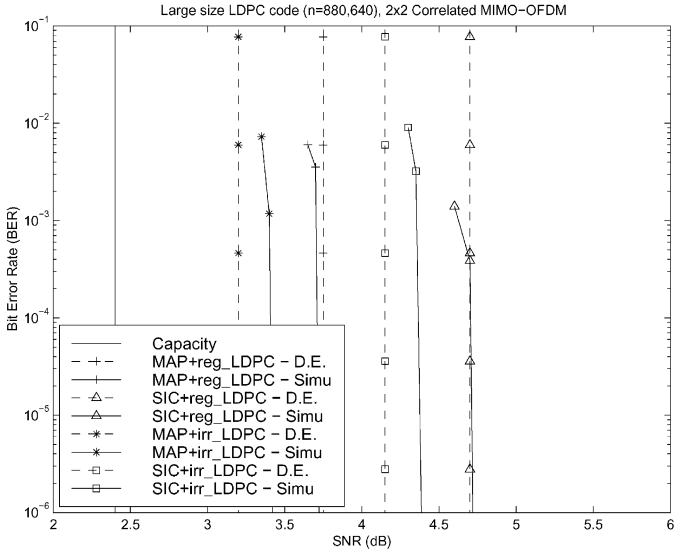

Fig. 7. Performance computed by density evolution analysis and computer simulations for ergodic 2×2 MIMO OFDM systems with spatial correlation.

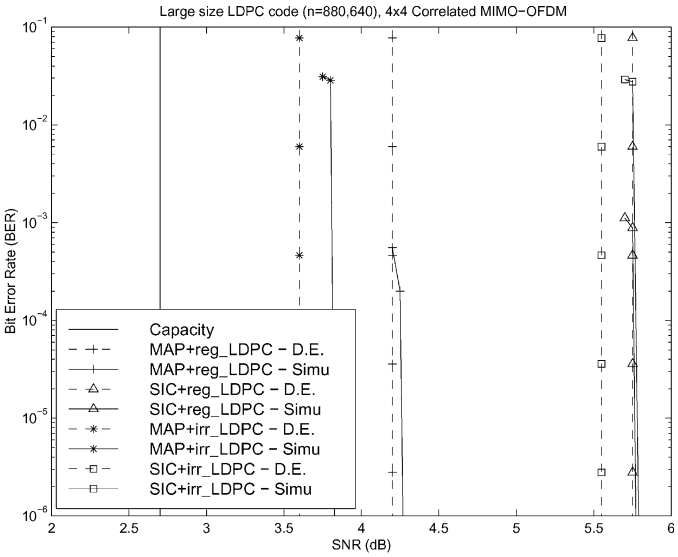

Fig. 8. Performance computed by density evolution analysis and computer simulations for ergodic 4×4 MIMO OFDM systems with spatial correlation.

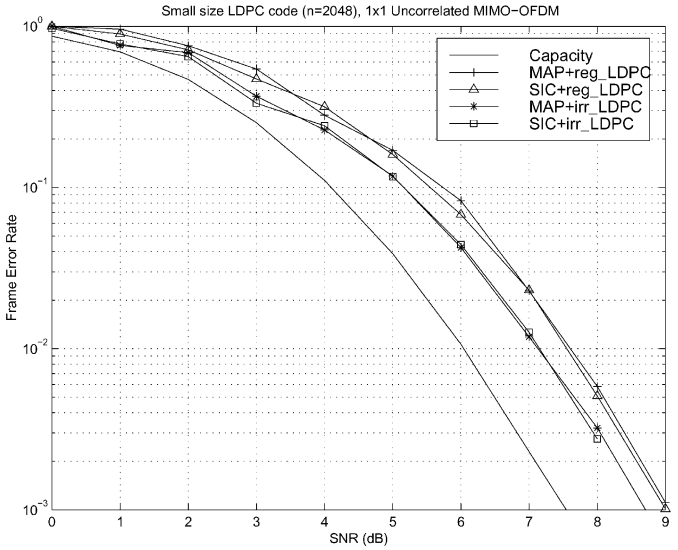

Fig. 9. Performance for outage 1×1 MIMO OFDM channels with no spatial correlation.

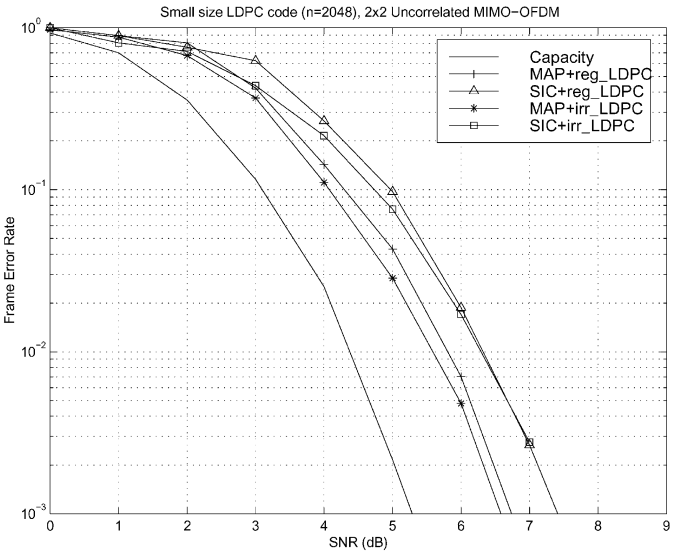

Fig. 10. Performance for outage 2×2 MIMO OFDM channels with no spatial correlation.

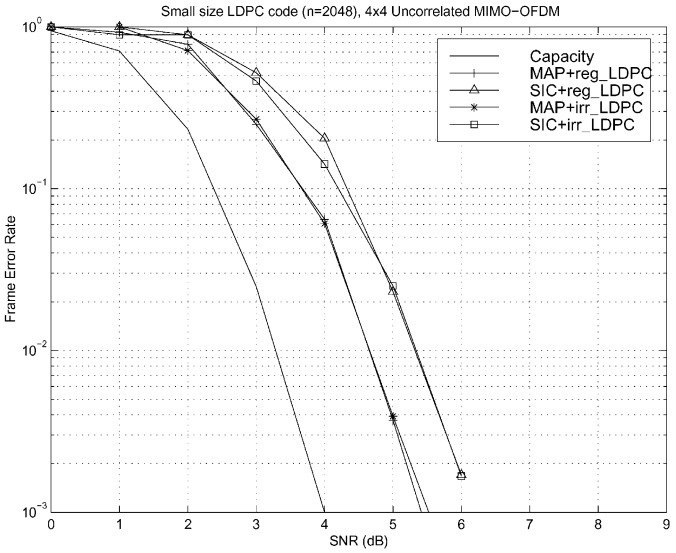

Fig. 11. Performance for outage 4×4 MIMO OFDM channels with no spatial correlation.

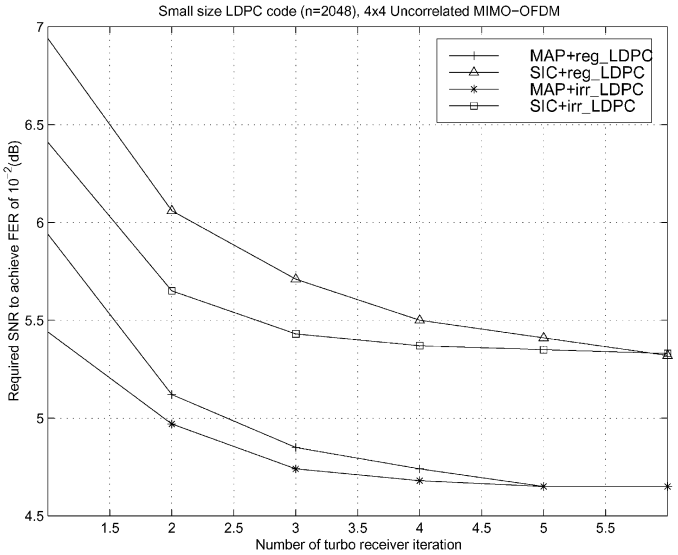

Fig. 12. For short block-size LDPC codes in 4×4 MIMO OFDM systems with no spatial correlation, the performance is plotted as the required SNR (in decibels) to achieve the FER of 10^{-2} versus the number of turbo receiver iteration. Note that flatter curves indicate faster receiver convergence.

iterative receiver can yield a performance within 1 dB from the capacity of correlated channels. This demonstrates again the generality and efficacy of the methods of density evolution with mixture Gaussians in optimizing LDPC OFDM MIMO systems. However, compared wiht the corresponding result in spatially uncorrelated channels (4×4 systems in particular), the performance of the LMMSE-SIC based receivers is degraded. We conjecture that the correlation matrices $\boldsymbol{R}_l$ and $\boldsymbol{S}_l$ lead to a larger matrix conditional number of $\boldsymbol{H}$ than it in uncorrelated MIMO channels, and therefore, the matrix operations (e.g., matrix inverse) in the LMMSE-SIC are more subject to numerical instability. (It is possible that some signal processing techniques are used to alleviate this issue; further discussion is beyond the scope of this paper.)

D. Small Block-Size LDPC-Coded MIMO OFDM

Thus far, we have focused on the design and optimization of the LDPC MIMO OFDM systems aiming to achieve the ergodic capacity. In doing so, large block-size LDPC codes were employed for the following reasons.

1) In order to achieve the ergodic channel capacity, the LDPC code word must be long enough to experience a very large number of fading channel realizations.
2) The results of the density evolution analysis are based on the assumption that extrinsic messages connected to each check node and variable node are independent, which holds valid when LDPC code block-size is very large.
3) In the procedure of the density evolution analysis and design, optimized degree profiles $\lambda(x)$ and $\rho(x)$ are first obtained, from which irregular LDPC codes are then randomly constructed. According to the theorem of concentration around ensemble average and the theorem of convergence to cycle-free ensemble average [26], such randomly constructed LDPC codes are guaranteed to have vanishing probability of error above the $\text{SNR}_{min.op}$

TABLE I
MISMATCH STUDY TO DEMONSTRATE THE REWARD OF CHANNEL-MATCHING IRREGULAR LDPC DESIGN. THE PERFORMANCE IS OBTAINED THROUGH SIMULATIONS IN THE SPATIAL-UNCORRELATED MIMO OFDM CHANNELS. *LDPC.I* DENOTES THE IRREGULAR LDPC CODES OPTIMIZED FOR THE CORRESPONDING MIMO OFDM CHANNELS; *LDPC.II* DENOTES THE IRREGULAR LDPC CODES ORIGINALLY DESIGNED FOR AWGN CHANNELS. THE PERFORMANCE (SNR) OF THE SHORT BLOCK LDPC-CODED MIMO OFDM IS MEASURED AT FER OF 10^{-2}

	Large Block Irregular LDPC			Small Block Irregular LDPC		
SNR (dB)	LDPC.I	LDPC.II	Channel-specific Design Gain (LDPC.II - LDPC.I)	LDPC.I	LDPC.II	Channel-specific Design Gain (LDPC.II - LDPC.I)
MAP (1×1)	2.57	2.57	0.00	7.08	7.08	0.00
MAP (2×2)	2.56	2.61	0.05	5.57	5.72	0.15
MAP (4×4)	2.46	2.65	0.19	4.48	4.81	0.33
SIC (1×1)	2.52	2.52	0.00	7.06	7.06	0.00
SIC (2×2)	2.75	2.92	0.17	6.32	6.44	0.12
SIC (4×4)	2.82	3.17	0.35	5.33	5.70	0.37

threshold (corresponding to the optimized $\lambda(x)$ and $\rho(x)$) when its code block-size is very large.

In reality, however, the price paid for achieving the ergodic channel capacity (or error-free communications) by employing very large block-size codes is large decoding delay. Usually, if small amount of fading outage is tolerable, it is a more common practice to employ a small block-size LDPC code, which spans a small number of fading channel states. The sensible performance measure accordingly is outage capacity [see (4)]. Unlike that for the ergodic channels, a systematic way of designing small block-size LDPC codes to achieve the outage channel capacity is so far unknown to the best of our knowledge; instead, a heuristic design approach that claims no theoretical optimality is adopted here. The design begins with the degree profiles that have been optimized above for the ergodic channels (i.e., $\tilde{n} \rightarrow \infty$). Based on these degree profiles, a small block-size LDPC code is randomly constructed by trial-and-error; more specifically, we drop the constructed LDPC codes with small girths in the bipartite graph, which to some extent leads to error-floor in FER performance. (It is also possible to construct small block-size LDPC codes by other methods, e.g., the method of bit-filling [30].)

The heuristically constructed small block-size LDPC codes ($n = 2048$) are simulated in outage MIMO OFDM channels ($\tilde{n} = 1$). In Figs. 9–11, the performance of regular and irregular LDPC codes when employed in systems with a different number of antennas and different types of demodulators is presented. Similar to the conclusions we drew above in ergodic channels, the proposed LDPC-coded MIMO OFDM systems can achieve both information rate increase and performance improvement when using multiple antennas; the MAP demodulator-based iterative receiver can perform within 1.5 dB from the outage capacity, and the low-complexity LMMSE-SIC demodulator-based receiver incurs additional small performance loss (< 1 dB) . In addition, in order to demonstrate the process of receiver convergence, we present the results in Figs. 9–11 in another form in Fig. 12, namely, the required SNR (in decibels) to achieve a FER of 10^{-2} versus the number of turbo receiver iteration. In a spatially uncorrelated 4×4 MIMO OFDM system, for both the MAP and the LMMSE-SIC demodulator-based receivers, we see that although the performance difference between regular and irregular LDPC codes after receiver convergence (the curve "Iter#6") is negligible, the irregular LDPC codes help to speed up the receiver convergence. Around 0.5 dB gain is achieved after the first receiver iteration for both the MAP and the LMMSE-SIC demodulator-based receiver. This observation suggests another benefit of optimizing LDPC codes, that is, to help reduce the number of receiver iterations and, consequently, the receiver complexity in the outage MIMO OFDM channels.

E. Mismatch Study

In the above, the performance of the optimized LDPC-coded MIMO OFDM is demonstrated, with LDPC codes being optimized for specific MIMO channels. As suggested by one reviewer, it is of certain interest to exhibit the reward of the channel-specific LDPC code design by comparing the performance of the MIMO-channel-optimized irregular LDPC codes with that of the AWGN-channel-optimized irregular LDPC codes in MIMO OFDM channels. The results are shown in Table I. In general, the channel-specific design gain increases for systems with a larger number of antennas. In addition, in outage channels, a good AWGN-optimized irregular LDPC code also exhibits the faster convergence of turbo iterative receiver than the nonoptimized regular LDPC codes. (The simulation curves are omitted here due to space limitations.)

VI. CONCLUSIONS

In this paper, we have considered the performance analysis and design optimization of LDPC-coded MIMO OFDM systems for high data-rate wireless transmission. The tools of density evolution with mixture Gaussian approximations have been used to optimize irregular LDPC codes and to compute minimum operational signal-to-noise ratios for ergodic MIMO OFDM channels. Furthermore, based on the LDPC profiles that were already optimized for ergodic channels, we also heuristically constructed small block-size irregular LDPC codes for outage MIMO OFDM channels. Several main conclusions are as follows.

1) Based on the optimized irregular LDPC codes, a turbo iterative receiver that consists of a soft maximum *a*

posteriori (MAP) demodulator and a belief-propagation LDPC decoder can perform within 1 dB above the ergodic channel capacity for various system configurations under consideration.

2) Likewise, based on the heuristically constructed small block-size irregular LDPC codes, a turbo iterative receiver based on MAP demodulator can perform within 1.5 dB above the outage channel capacity.
3) Compared with the receiver employing the MAP demodulator, the receiver employing a low-complexity linear minimum mean-square-error soft-interference-cancellation (LMMSE-SIC) demodulator has limited performance loss (less than 1 dB) in spatially uncorrelated channels but suffers extra performance loss in spatially correlated channels.
4) In ergodic MIMO OFDM channels, the optimization gain of the irregular LDPC codes over the regular LDPC codes tends to be smaller for systems with larger number of antennas. In outage MIMO OFDM channels, both the regular and irregular LDPC codes perform close to each other for systems with a larger number of antennas after the receiver converges; however, the irregular LDPC codes are helpful to expedite the convergence of iterative receiver.

REFERENCES

[1] P. Bender, P. Black, M. Grob, R. Padovani, N. Sindhushyana, and S. Viterbi, "CDMA/HDR: A bandwidth efficient high speed wireless data service for nomadic users," *IEEE Commun. Mag.*, vol. 38, pp. 70–77, July 2000.

[2] G. J. Foschini, "Layered space-time architecture for wireless communication in a fading environment when using multi-element antennas," *Wireless Pers. Commun.*, vol. 1, pp. 41–59, 1996.

[3] S. M. Alamouti, "A simple transmit diversity technique for wireless communications," *IEEE J. Select. Areas Commun.*, vol. 16, pp. 1451–1458, Oct. 1998.

[4] V. Tarokh, N. Seshadri, and A. R. Calderbank, "Space-time codes for high data rate wireless communication: Performance criterion and code construction," *IEEE Trans. Inform. Theory*, vol. 44, pp. 744–765, Mar. 1998.

[5] İ. E. Telatar, "Capacity of multi-antenna gaussian channels," *Eur. Trans. Telecommun.*, vol. 10, pp. 585–595, Nov.–Dec. 1999.

[6] B. Lu, X. Wang, and K. R. Narayanan, "LDPC-based space-time coded OFDM systems over correlated fading channels," *IEEE Trans. Commun.*, vol. 50, pp. 74–88, Jan. 2002.

[7] S. ten Brink, G. Kramer, and A. Ashikhmin, "Design of low-density parity-check codes for multi-antennas modulation and detection," *IEEE Trans. Commun.*, submitted for publication.

[8] G. J. Foschini and M. J. Gans, "On limits of wireless communications in a fading environment when using multiple antennas," *Wireless Pers. Commun.*, vol. 6, pp. 311–335, Mar. 1998.

[9] D. Shiu, G. J. Foschini, M. J. Gans, and J. M. Kahn, "Fading correlation and its effect on the capacity of multi-element antenna systems," in *Proc. Universal Pers. Commun. Conf.*, Oct. 1998.

[10] E. Biglieri, G. Taricco, and A. Tulino, "Performance of space-time codes for a large number of antennas," *IEEE Trans. Inform. Theory*, vol. 48, pp. 1794–1803, July 2002.

[11] B. Hassibi and B. Hochwald, "High-rate codes that are linear in space and time," IEEE Trans. Inform. Theory, vol. 48, pp. 1804–1824, July 2002, submitted for publication.

[12] S.-Y. Chung, G. D. Forney, T. J. Richardson, and R. Urbanke, "On the design of low-density parity-check codes within 0.0045 dB of the shannon limit," *IEEE Commun. Lett.*, vol. 52, pp. 58–60, Feb. 2001.

[13] M. G. Luby, M. Mitzenmacher, M. A. Shokrollahi, and D. A. Spielman, "Analysis of low density codes and improved designs using irregular graphs," in *Proc. 30th ACM Symp. Theory Comput.*, 1998.

[14] T. J. Richardson and R. L. Urbanke, "Capacity of low density parity check codes under message passing decoding," *IEEE Trans. Inform. Theory*, vol. 47, pp. 599–618, Feb. 2001.

[15] K. R. Narayanan, X. Wang, and G. Yue, "LDPC code design for MMSE turbo equalization," in *Proc. IEEE Int. Symp. Information Theory*, Lausanne, Switzerland, June 2002.

[16] H. Bölcskei, D. Gesbert, and A. J. Paulraj, "On the capacity of OFDM-based spatial multiplexing systems," *IEEE Trans. Commun.*, pp. 225–234, Feb. 2002.

[17] G. Ungerboeck, "Channel coding with multilevel/phase signals," *IEEE Trans. Inform. Theory*, vol. IT-28, pp. 55–67, Jan. 1982.

[18] X. Wang and H. V. Poor, "Iterative (Turbo) soft interference cancelation and decoding for coded CDMA," *IEEE Trans. Commun.*, vol. 47, pp. 1046–1061, July 1999.

[19] J. Hagenauer, E. Offer, C. Meason, and M. Morz, "Decoding and equalization with analog nonlinear networks," *Eur. Trans. Telecommun.*, pp. 389–400, Oct. 1999.

[20] H. E. Gamal and A. R. Hammons, "Analyzing the turbo decoder using the Gaussian assumption," *IEEE Trans. Inform. Theory*, vol. 47, pp. 671–686, Feb. 2001.

[21] S. ten Brink, "Convergence of iterative decoding," *Electron. Lett.*, pp. 1117–1118, June 1999.

[22] E. Lehmann and G. Casella, *Theory of Point Estimation*, 2 ed. New York: Springer-Verlag, 1998.

[23] G. J. McLachlan and T. Krishnan, *The EM Algorithm and Extensions*. New York: Wiley, 1997.

[24] P. McKenzie and M. Alder, "Selecting the optimal number of components for a gaussian mixture model," in *Proc. IEEE Int. Symp. Inform. Theory*, 1994.

[25] J. Rissanen, *Stochastic Complexity in Statistical Inquiry*. Singapore: World Scientific, 1989.

[26] T. J. Richardson, M. A. Shokrollahi, and R. L. Urbanke, "Design of capacity-approaching irregular low-density parity-check codes," *IEEE Trans. Inform. Theory*, vol. 47, pp. 619–637, Feb. 2001.

[27] K. Price and R. Storn, "Differential evolution—a simple and efficient heuristic for global optimization over continuous spaces," *J. Global Optim.*, vol. 11, pp. 341–369, 1997.

[28] D. J. C. MacKay and R. M. Neal, "Near shannon limit performance of low density parity check codes," *Electron. Lett.*, vol. 33, pp. 457–458, Mar. 1997.

[29] M. Stege, M. Bronzel, and F. Fettweis, "MIMO-capacities for COST 259 scenarios," in *Proc. Int. Zurich Seminar Broadband Commun.*, Feb. 2002.

[30] J. Campello, D. S. Modha, and S. Rajagopalan, "Designing LDPC codes using bit-filling," in *Proc. IEEE Int. Conf. Commun.*, Oct. 2001, pp. 55–59.

Ben Lu (M'02) received the B.E. and M.S. degrees in electrical engineering from Southeast University, Nanjing, China, in 1994 and 1997 and the Ph.D. degree from Texas A&M University, College Station, in 2002.

From 1994 to 1997, he was a research assistant with National Mobile Communications Research Laboratory, Southeast University. From 1997 to 1998, he was with the CDMA Research Department, Zhongxing Telecommunication Equipment Co., Shanghai, China. He worked as a Member of Technical Staff with Santel Networks, Newark, CA, in 2002. Since August 2002, he has been with NEC Laboratories America, Princeton, NJ. His research interests include the signal processing and error-control coding for mobile and wireless communication systems.

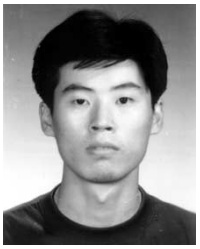

Guosen Yue (S'04) received the B.S. degree in physics and the M.S. degree in electrical engineering from Nanjing University, Nanjing, China in 1994 and 1997, respectively. He is currently pursuing the Ph.D. degree with the Department of Electrical Engineering, Texas A&M University, College Station.

His research interests are in the area of telecommunications and digital signal processing, primarily in channel coding and modulation for wireless communications.

Xiaodong Wang (M'98) received the B.S. degree in electrical engineering and applied mathematics (with the highest honor) from Shanghai Jiao Tong University, Shanghai, China, in 1992, the M.S. degree in electrical and computer engineering from Purdue University, West Lafayette, IN, in 1995, and the Ph.D degree in electrical engineering from Princeton University, Princeton, NJ, in 1998.

From July 1998 to December 2001, he was an Assistant Professor with the Department of Electrical Engineering, Texas A&M University, College Station. In January 2002, he joined the Department of Electrical Engineering, Columbia University, New York, NY, as an Assistant Professor. His research interests fall in the general areas of computing, signal processing, and communications. He has worked in the areas of digital communications, digital signal processing, parallel and distributed computing, nanoelectronics, and bioinformatics and has published extensively in these areas. His current research interests include wireless communications, Monte Carlo-based statistical signal processing, and genomic signal processing.

Dr. Wang received the 1999 NSF CAREER Award and the 2001 IEEE Communications Society and Information Theory Society Joint Paper Award. He currently serves as an Associate Editor for the IEEE TRANSACTIONS ON COMMUNICATIONS, the IEEE TRANSACTIONS ON WIRELESS COMMUNICATIONS, the IEEE TRANSACTIONS ON SIGNAL PROCESSING, and the *EURASIP Journal of Applied Signal Processing*.